



## OPEN ACCESS

## EDITED BY

Derek Keir,  
University of Southampton, United Kingdom

## REVIEWED BY

Huan Li,  
Central South University, China  
Chang-Hao Xiao,  
Institute of Geomechanics Chinese Academy  
of Geological Sciences, China

## \*CORRESPONDENCE

Weicui Ding,  
✉ dingweicui@163.com  
Feizhou Ma,  
✉ mfeizhou@mail.cgs.gov.cn

RECEIVED 17 July 2024

ACCEPTED 20 January 2025

PUBLISHED 25 February 2025

## CITATION

Xu S, Ding W, Ma F, Chen X, Shao Z, Han L,  
Huang P, Shi J and Yang X (2025) Deep crustal  
composition and Late Paleozoic geotectonic  
evolution in West Junggar, China.  
*Front. Earth Sci.* 13:1465894.  
doi: 10.3389/feart.2025.1465894

## COPYRIGHT

© 2025 Xu, Ding, Ma, Chen, Shao, Han,  
Huang, Shi and Yang. This is an open-access  
article distributed under the terms of the  
[Creative Commons Attribution License \(CC  
BY\)](https://creativecommons.org/licenses/by/4.0/). The use, distribution or reproduction in  
other forums is permitted, provided the  
original author(s) and the copyright owner(s)  
are credited and that the original publication  
in this journal is cited, in accordance with  
accepted academic practice. No use,  
distribution or reproduction is permitted  
which does not comply with these terms.

# Deep crustal composition and Late Paleozoic geotectonic evolution in West Junggar, China

Shenglin Xu<sup>1</sup>, Weicui Ding<sup>1\*</sup>, Feizhou Ma<sup>1,2\*</sup>, Xuanhua Chen<sup>1</sup>,  
Zhaogang Shao<sup>1</sup>, Lele Han<sup>1</sup>, Penghui Huang<sup>1,3</sup>, Jianjie Shi<sup>1</sup> and  
Xinru Yang<sup>1</sup>

<sup>1</sup>SinoProbe Center, Chinese Academy of Geological Sciences and China Geological Survey, Beijing, China, <sup>2</sup>China Geological Survey, Beijing, China, <sup>3</sup>Beijing Research Institute of Geological Engineering Design, Beijing, China

The West Junggar area in the southwestern part of the Central Asian Orogenic Belt (CAOB), is one of the largest areas of growth of the Phanerozoic crust in the world that has experienced intense Late Paleozoic magmatic activity, where crust-mantle interaction is significant. The issue of crustal growth has long been regarded as one of the most fundamental in earth sciences. In light of the challenges posed by the composition of deep materials and the Late Paleozoic crustal growth in the West Junggar area, there is a continued need to systematically determine the spatial distribution characteristics of deep materials in the crust, analysis the growth pattern and growth volume of the crust, and enhance the Late Paleozoic tectonic evolution of the region. Focusing on granite type Sr-Nd-Pb-Hf isotopic mapping, this study found that the West Junggar area has the isotopic characteristics of high positive  $\epsilon_{\text{Hf}}(t)$  and  $\epsilon_{\text{Nd}}(t)$ , low (87 Sr/86 Sr)<sub>i</sub>, and young crustal mode age, there is almost no old crystalline basement in the deep crust. During the Late Paleozoic, about 85% of West Junggar had 75%–95% crustal growth, dominated by lateral crustal growth and material recirculation; about 15% of the area (connected to the Jietebudiao area) had 50%–75% crustal growth, dominated by vertical crustal growth. The West Junggar area mainly experienced four orogenic stages in the Late Paleozoic. In the Early Carboniferous period (360–320 Ma), there was significant intra-oceanic subduction, involving a substantial amount of juvenile material in lateral crustal accretion. The Late Carboniferous-Early Permian period (320–294 Ma) is the post-orogenic extension stage, during which a massive amount of juvenile mantle source was added. This resulted in the most intense magmatism and crustal growth, which could have the growth of the crust potentially more than 75%. In the Early Permian period (294–272 Ma), there was an intracrustal evolution stage and a decrease in the participation of juvenile material. During the Early Permian-Early Triassic period (272–250 Ma), magmatic activity decreased significantly, where the southwestern region experienced high-temperature, low-pressure, crustal thinning extension. Despite this, the crust received juvenile material, and plutonic magma intrusion occurred.

## KEYWORDS

Late Paleozoic, Sr-Nd-Pb-Hf mapping, material composition, crustal growth, geotectonic evolution, West Junggar

## 1 Introduction

Isotopic tracing is a crucial tool for chemical geodynamic studies. It is one of the most important methods for analyzing the evolutionary history of the crust and mantle, identifying the material composition of the lithosphere, and exploring the deep dynamical processes of the Earth (Zheng et al., 1998; Wang and Hou, 2018; Hou and Wang, 2018). Isotopic mapping focuses on the continental lithosphere, using regional magmatic isotope data to reveal deep material composition and explore tectonic boundaries. This provides important support for understanding the growth of the continental crust and the tectonic evolution.

CAOB is one of the largest accretionary orogenic belts in the world, spanning over 5,000 km from the Siberian Craton to the European Craton and the North China Craton (Xiao et al., 2012; Chen et al., 2012a, Chen et al., 2012b, Chen et al., 2013a, Chen et al., 2016, Chen et al., 2022; Lkhagvasuren et al., 2020; Li et al., 2017; Sun et al., 2017; Wu et al., 2017; Yang et al., 2023; Yang et al., 2024) as a giant suture zone (Figure 1A). During the Late Paleozoic, the western part of the CAOB experienced significant crust-mantle interactions. This led to the development of numerous high-magnesium andesites, island-arc granites, adakite, and picrite, which are important indicators of regional oceanic crustal subduction (Zhang and Huang, 1992; Buslov et al., 2004). As an important component of the western section of the CAOB (Figure 1B), the Phanerozoic's crustal growth is of particular significance, and research findings are abundant (Shen et al., 2015; Jahn, 2004; Chen et al., 2014; Xu et al., 2022a; Liu et al., 2023). The crustal growth during the Late Paleozoic is manifested as follows: ① The crust exhibits significant lateral and vertical accretion and has a multi-stage evolutionary process. ② There is an intense interaction between the crust and mantle, with clear material cycling and multi-rotation characteristics (Han et al., 1998; Han et al., 2006; Zhu Y. F et al., 2007; Xiao et al., 2008; Xu et al., 2019a).

The studies on CAOB have shown that the Phanerozoic crustal growth may exceed 50% and is one of the most significant Phanerozoic crustal growth regions in the world (Huang et al., 2018; Wang and Hou, 2018). Some scholars have expressed differing views (Liu and Nie, 2015; Lv et al., 2017).

In the past, research on the source areas and crustal growth of magmatism in the West Junggar area has been carried out by different types of magmatism, resulting in a substantial accumulation of research information. However, the spatial distribution characteristics of deep crustal materials, the delineation of isotopic crustal boundaries in the region, and the quantitative-semi-quantitative estimation of crustal growth have not been systematically analyzed, resulting in a pattern of crustal growth in the West Junggar area that still needs to be studied in depth. Xu et al. (2022a) conducted Sr-Nd-Pb isotope studies in the West Junggar area. This paper combines their research results with the extensive collection of Hf isotope data published by previous authors (Chen S. S. et al., 2013; Yin et al., 2016; Jiang et al., 2015; Wang et al., 2017; Yang et al., 2015; Jin et al., 2016; Tian and Yang, 2015; Geng et al., 2009; Zhang and Zhang, 2014; Li et al., 2014; Li et al., 2015; Tang et al., 2012; Chen J. F. et al., 2015; Yin et al., 2015; Wu et al., 2018; Shen et al., 2017; Wang X. S. et al., 2018; Zhang et al.,

2018; Xu et al., 2019b; Xu et al., 2020; Xu et al., 2022b), has added the Hf isotope data for key areas in the study (Supplementary Table S1). It comprehensively explores the Sr-Nd-Pb-Hf isotopic composition of granite analogs in the West Junggar area. The Kriging interpolation method (Chen et al., 2007) has generated the Sr-Nd-Pb-Hf isotope contour maps in the Suffer 14 software. We combine with the regional tectonic background, analyze the composition of deep crustal materials, delineate the tectonic boundaries of the crust in the region, explore the amount of crustal growth, growth periods, and patterns, and explore the late Paleozoic tectonic evolution of West Junggar.

## 2 Regional geological background

### 2.1 Regional faults

The West Junggar Faults System is located between the Chenggis-Junggar Fault, the Tianshan Fault, and the Irtysh Strike-slip Fault (Figure 1B). The region is characterized by large-scale left or right lateral strike-slip faults (Chen et al., 2009; Chen et al., 2015; Han et al., 2019; Ding et al., 2020). The left-lateral strike-slip faults consist of three large-scale faults: the Darabut Fault, the Karamay Fault, and the Baerluke Fault. And a series of smaller-scale secondary faults. The right-lateral strike-slip faults are primarily composed of large-scale faults, including the Zalulshan-Labashan Fault and the Abbey Lake Fault (Figure 2).

### 2.2 Stratigraphy

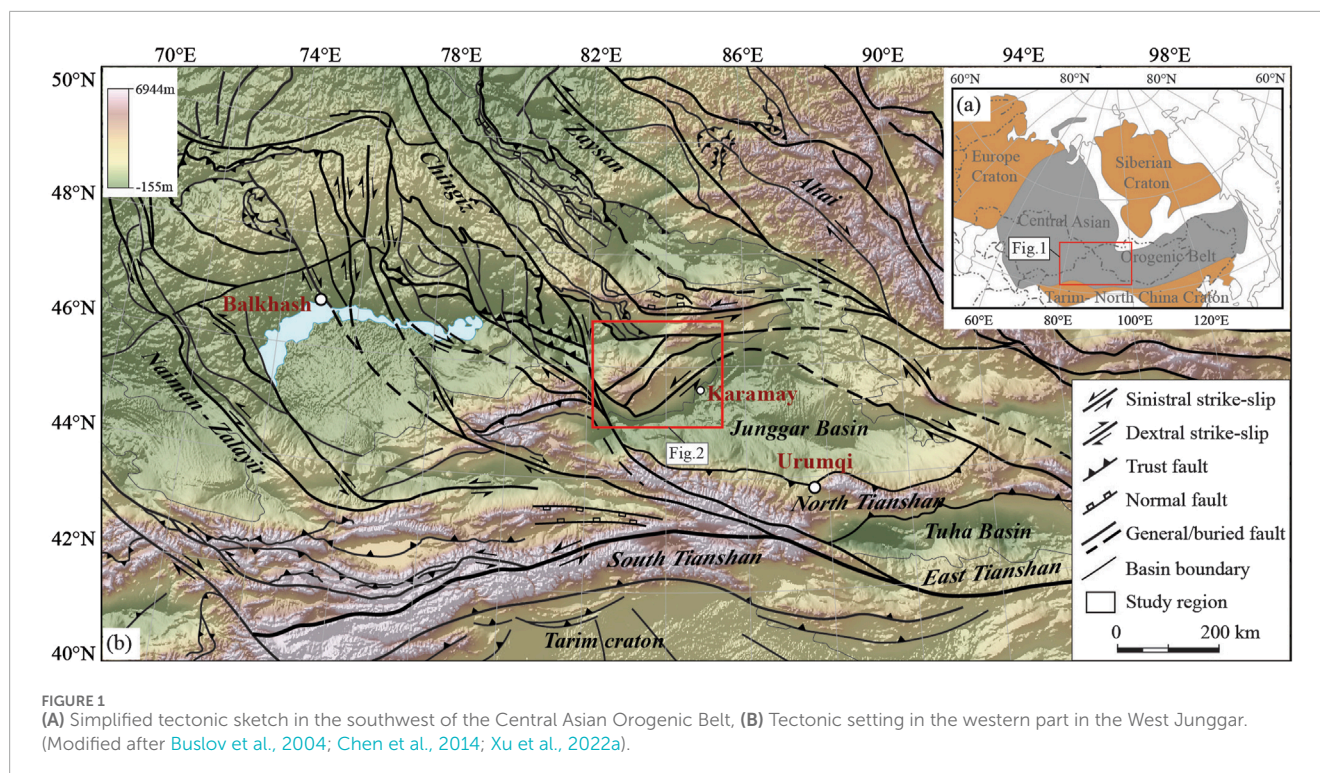
Sedimentary strata have been widely distributed in the West Junggar area since the Phanerozoic era, with the Paleozoic era being the most developed (He et al., 2004; Figure 2). The sedimentary strata can be divided into two parts: one is the Early Paleozoic metamorphic stratigraphy, which is dominated by flysch formation and ophiolite mélangé, with strong metamorphism and deformation; the other is the Late Paleozoic pyroclastic sedimentary formation, which consists of giant-thick marine-continental slope-face sedimentary rocks (Zhu et al., 2013).

### 2.3 Ophiolite mélangé

Regional ophiolite mélanges such as Darabut, Karamay, and Baerluke are distributed along the main fault zones (Figure 2). The rock compositions include serpentinite peridotite, dunite, serpentine, pyroxenite, gabbro, diabase, basalt, oceanic plagiogranite, and siliceous rocks.

### 2.4 Magmatism

The Late Paleozoic magmatic activity in the region was intense, with abundant rock types, divided into large granitic basement and small and medium-sized rock strains (Figure 2).



The granite basement comprises the Miaoergou, Kurumusu, Karamay, and Hatu batholiths. The rocks consist mainly of A-type granites, such as alkaline and monzonitic granite. These rocks are characterized by high silica, quasi-alumina-weak per aluminum, high-K calc-alkaline, low magnesium, and ferrum, which belong to the post-collisional orogenic stage of the Late Carboniferous-Early Permian (Han et al., 2006; Su et al., 2006; Zhou et al., 2008).

The small and medium-sized rock strains are dispersed, and the rocks consist mainly of granodiorite, biotite granite, quartz diorite, and diorite porphyrite.

These rocks may have formed during the Middle-Late Carboniferous subduction of the mid-ocean ridge or in the island arc environment, and some of the island arc granites have obvious adakite characteristics (Geng et al., 2009; Zhang et al., 2006; Tang et al., 2009; Tang et al., 2010a; Tang et al., 2010b; Shen et al., 2009).

### 3 Sample preparation and analytical methods

Based on the completion of the U-Pb dating of the sample zircon, the zircon Lu-Hf isotope analysis was carried out at the State Key Laboratory of Continental Dynamics of Northwestern University, where the location of the zircon Lu-Hf isotope measurement point and the location of the U-Pb dating measurement point is the same magmatic growth ring belt within the same zircon grain. The laser ablation system is a 193 nm excimer laser ablation system (RESOLUTION M-50, ASI) with a frequency of 5 Hz, a spot size of 43  $\mu\text{m}$ , and a carrier gas of high-purity helium.

Lu-Hf isotopes were analyzed by multi-reception plasma mass spectrometry (Nu Plas Ma II MC-ICPMS). During the analysis, international standard zircon samples 91,500 and Mud Tank were used as monitoring samples, and a set of international standard samples was inserted every 8 samples. The data acquisition mode was TRA mode with an integration time of 0.2 s, a background acquisition time of 30 s, a sample integration time of 50 s, and a purge time of 40 s. The specific test steps and methods are described in detail in Bao et al. (2017) and Yuan et al. (2008). Among them, the average value of  $^{176}\text{Hf}/^{177}\text{Hf}$  determination of standard sample 91,500 is  $0.282,313 \pm 0.000021$  ( $2\sigma$ ), and the average value of  $^{176}\text{Hf}/^{177}\text{Hf}$  determination of standard sample Mud Tank is  $0.282,524 \pm 0.000013$  ( $2\sigma$ ), and the test data of the standard samples are all within the error range (Yuan et al., 2008), indicating that the test results of the samples in this paper are reliable. The detailed test results are shown in Supplementary Appendix Table S2.

## 4 Regional isotope characterization

### 4.1 Sr-Nd-Pb isotopes characterization

The West Junggar area is characterized by higher ( $^{143}\text{Nd}/^{144}\text{Nd}$ )<sub>i</sub> values and positive  $\epsilon_{\text{Nd}}(t)$  values, with an overall range of  $\epsilon_{\text{Nd}}(t)$  values of 2.29–8.75, and an overall range of crustal model ages of 345–851 Ma (Xu et al., 2022a). The basement of the West Junggar region is dominated by juvenile crust (Figure 3). The Nd isotope maps show the distribution of isotope provinces, which are divided into three-high, three-medium, and one-low, with material sources from Paleoproterozoic,

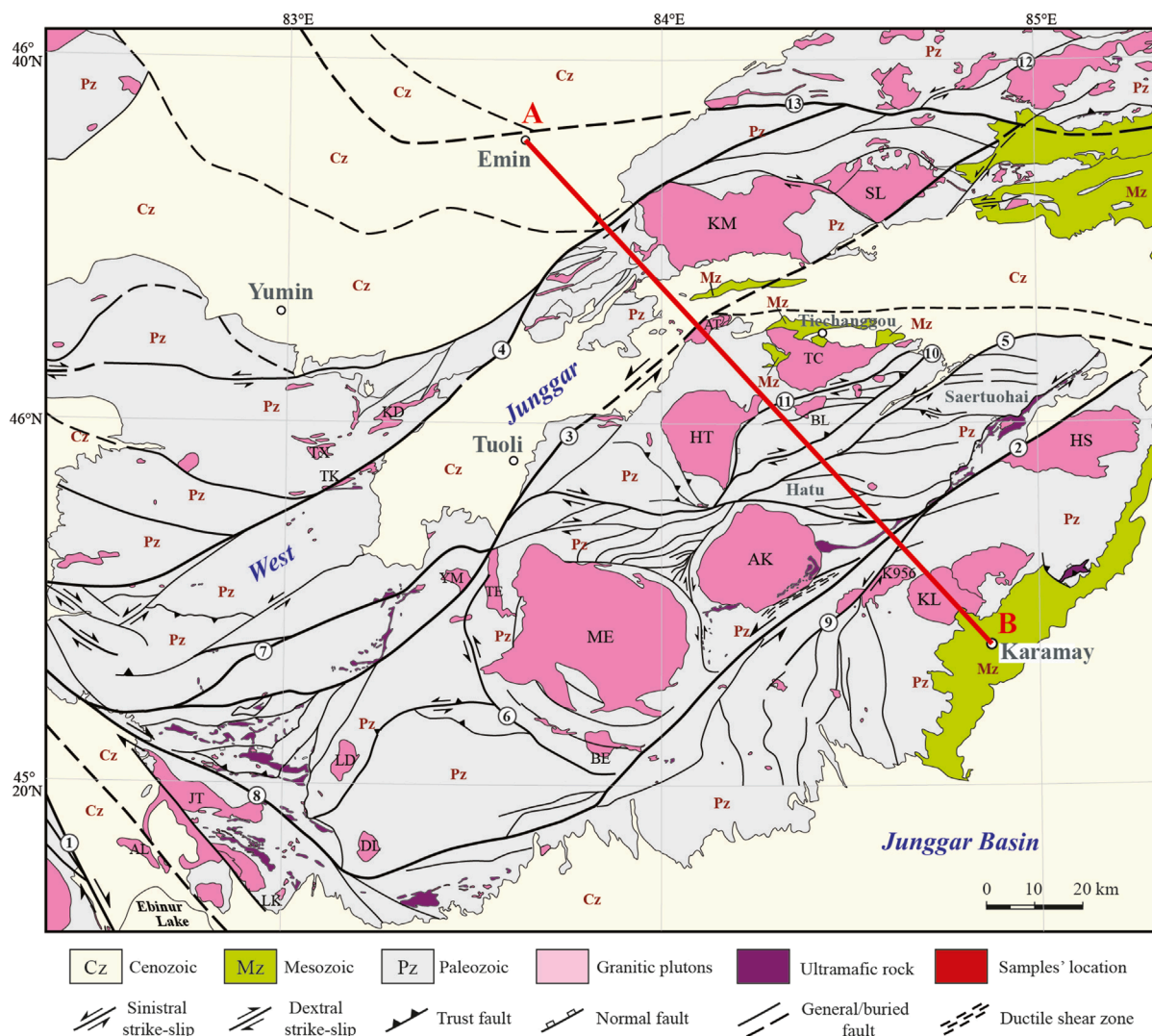


FIGURE 2 Stratigraphic, structure-magmatic diagram of the West Junggar Area. (A, B) shows the location of the profile in Figure 8. (Modified after Chen et al., 2011, Chen et al., 2015a, Chen et al., 2017).

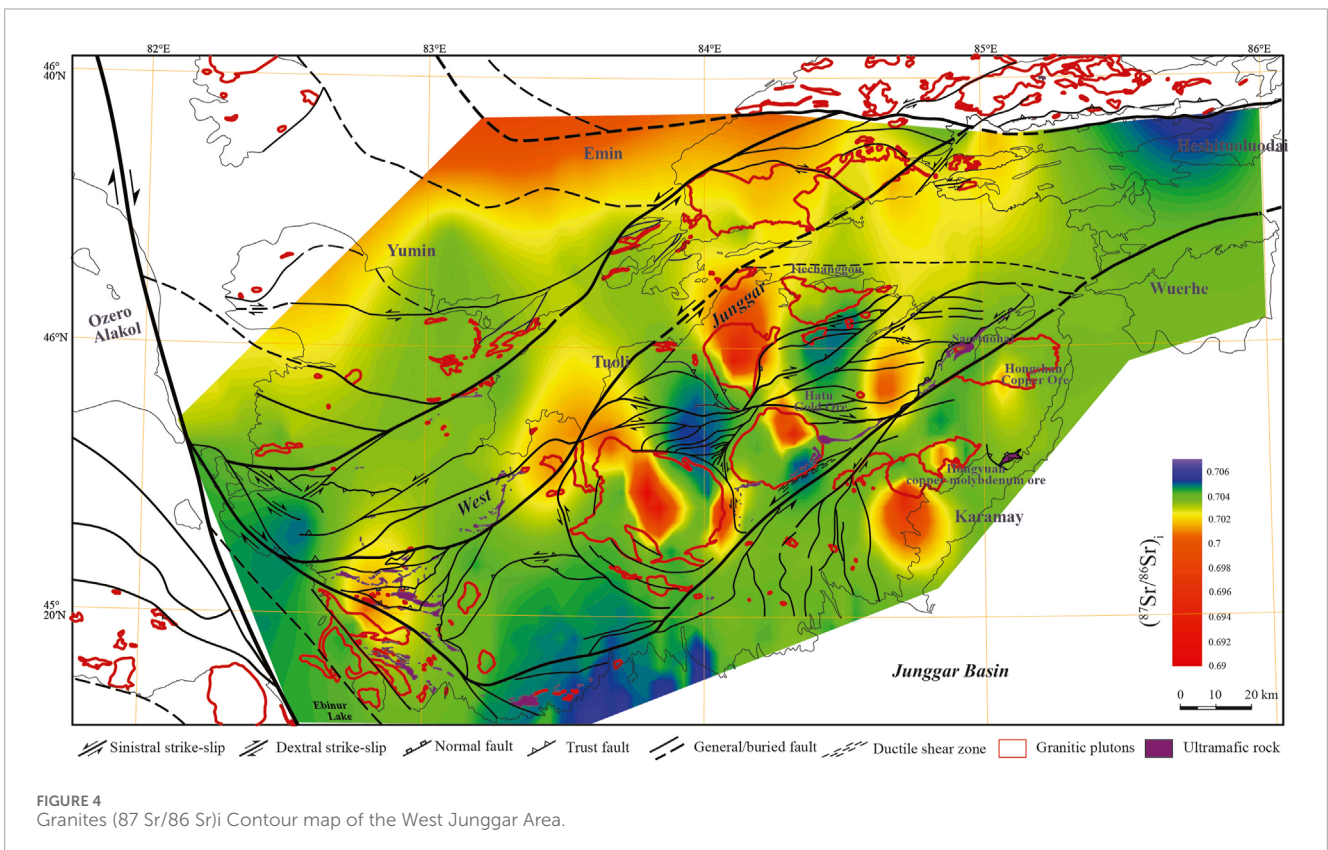
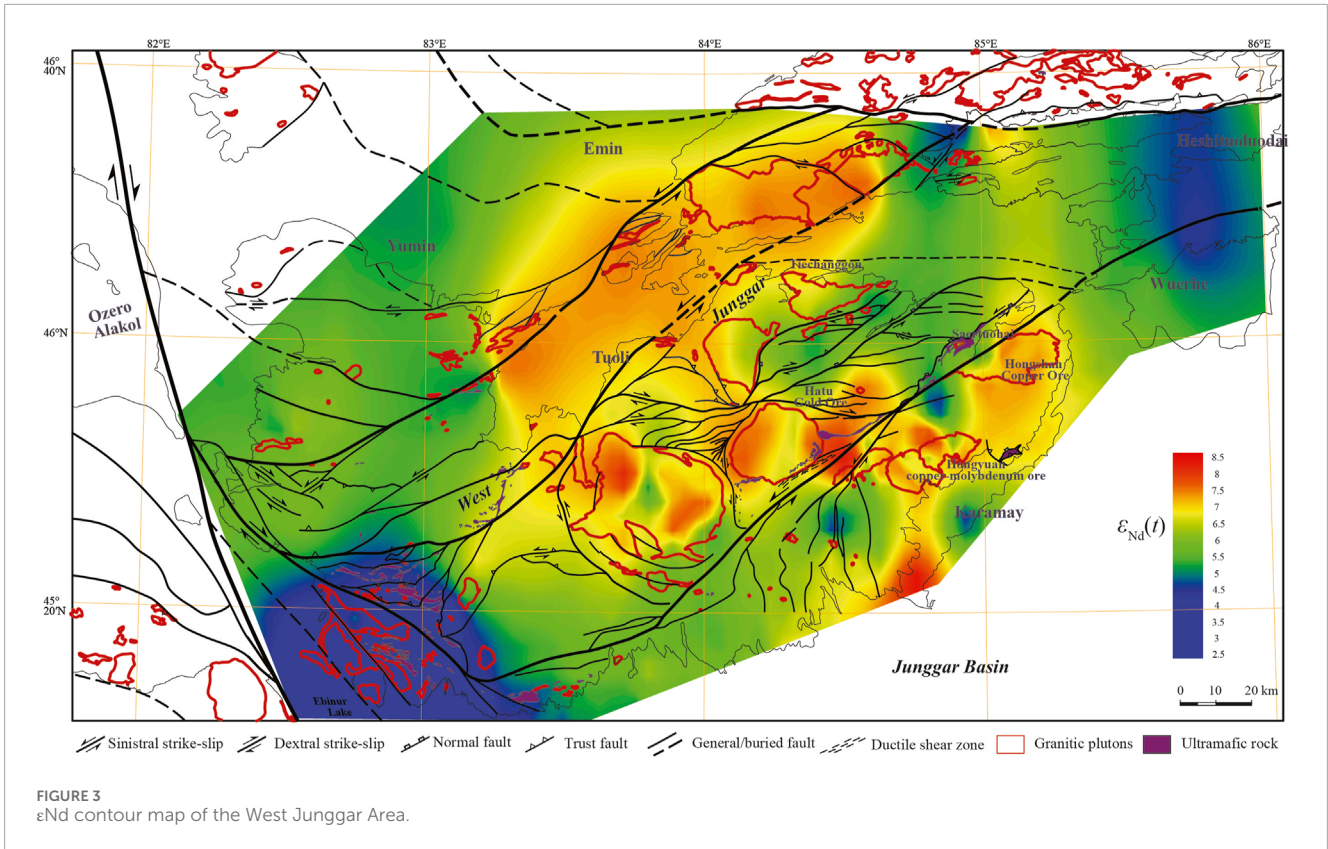
middle-late Neoproterozoic, and early Neoproterozoic material respectively.

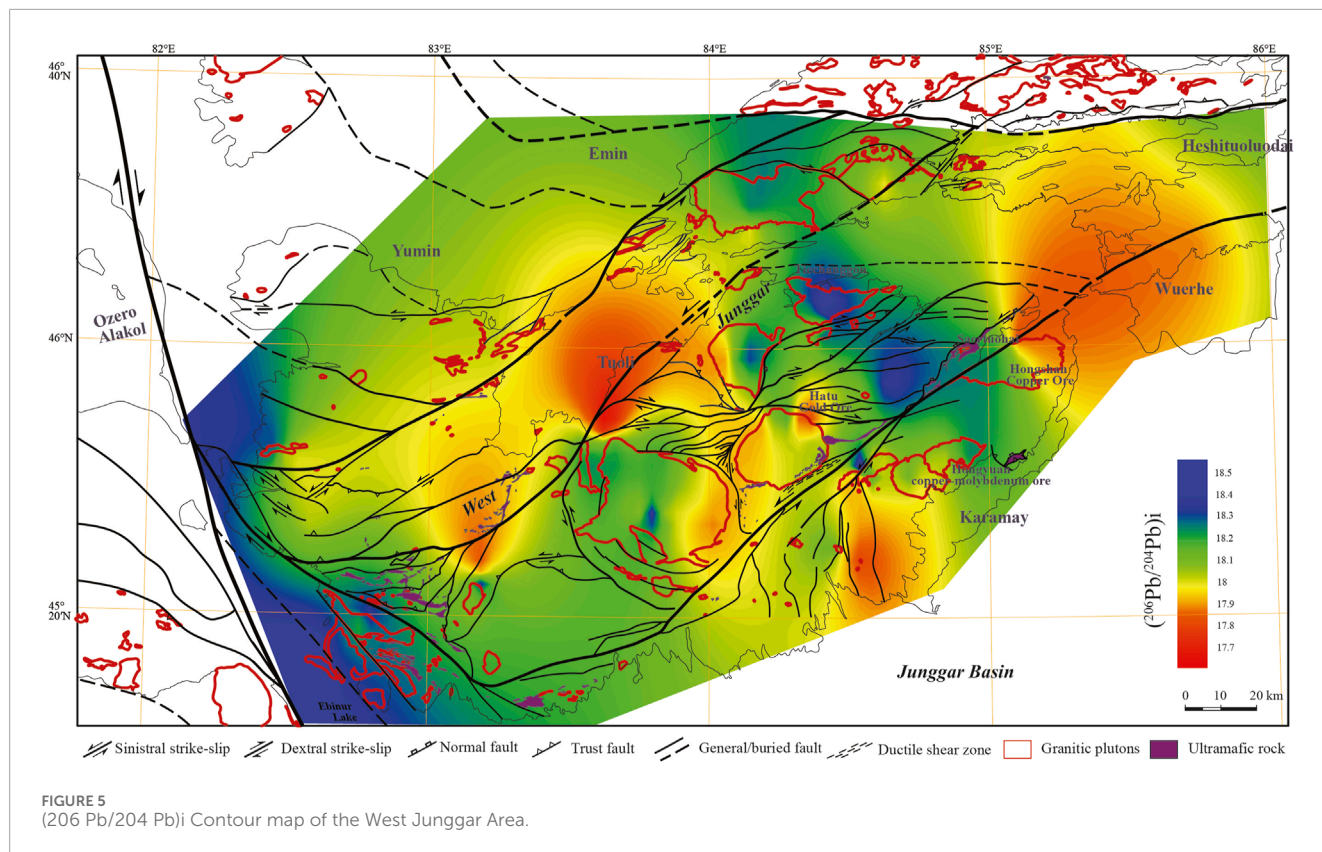
The isotopic ratio range for granites ( $^{87}\text{Sr}/^{86}\text{Sr}$ )<sub>i</sub> in the West Junggar region is considerably wide, spanning from 0.697,397 to 0.708,336, which is coupled with the Nd isotopic signatures (Xu et al., 2022a). The Sr isotopic characteristics also suggest that the crust of the West Junggar area mainly originated from the juvenile crust, with minimal ancient crustal material. The Sr isotope maps show the distribution characteristics, with ultra-low-value, low-value, and medium-low-value provinces (Figure 4).

The ratio range for ( $^{206}\text{Pb}/^{204}\text{Pb}$ )<sub>i</sub> of the West Junggar area spans from 17.4975 to 19.0352 (Xu et al., 2022a), indicating that the crust of the study region did not mixed the ancient crust during the Late Paleozoic magmatic intrusion process. The Pb isotope maps show the distribution characteristics, with high-value, medium-value, and low-value provinces (Figure 5).

## 4.2 Hf isotopic characterization

The West Junggar region is characterized by higher  $^{176}\text{Hf}/^{177}\text{Hf}$  ratios and positive  $\epsilon_{\text{Hf}}(t)$  values, with individual sample values displaying a broad range of variability. The overall mean range of  $\epsilon_{\text{Nd}}(t)$  values and crustal model ages are 6.67–16.82 and 251–893 Ma respectively. The minimum value of  $\epsilon_{\text{Hf}}(t)$  ranges from 2.79 to 14.49, and the maximum value of crustal model age is 425–1,148 Ma. The crust of the West Junggar area is mainly juvenile crust, which can be divided into three levels of Hf isotope provinces (Figure 6): High  $\epsilon_{\text{Hf}}$  value province, Medium  $\epsilon_{\text{Hf}}$  value province, and Low  $\epsilon_{\text{Hf}}$  value provinces. The high  $\epsilon_{\text{Hf}}$  values provinces are mainly distributed in the numerous rock masses proximal to the Darabut Fault and the partial rock mass of the north-central segment in the Mayile Fault. The Medium  $\epsilon_{\text{Hf}}$  value province is mainly distributed in the area around the Tiechanggou batholith-western Miaoergou batholith-Labahedong





batholith. The northwest of Karamay, south of Tiechanggou batholith, near Tuoli County, and the Jietebudiao batholith exhibit relatively low  $\epsilon_{\text{Hf}}$  values.

## 5 Discussion

### 5.1 Deep material composition

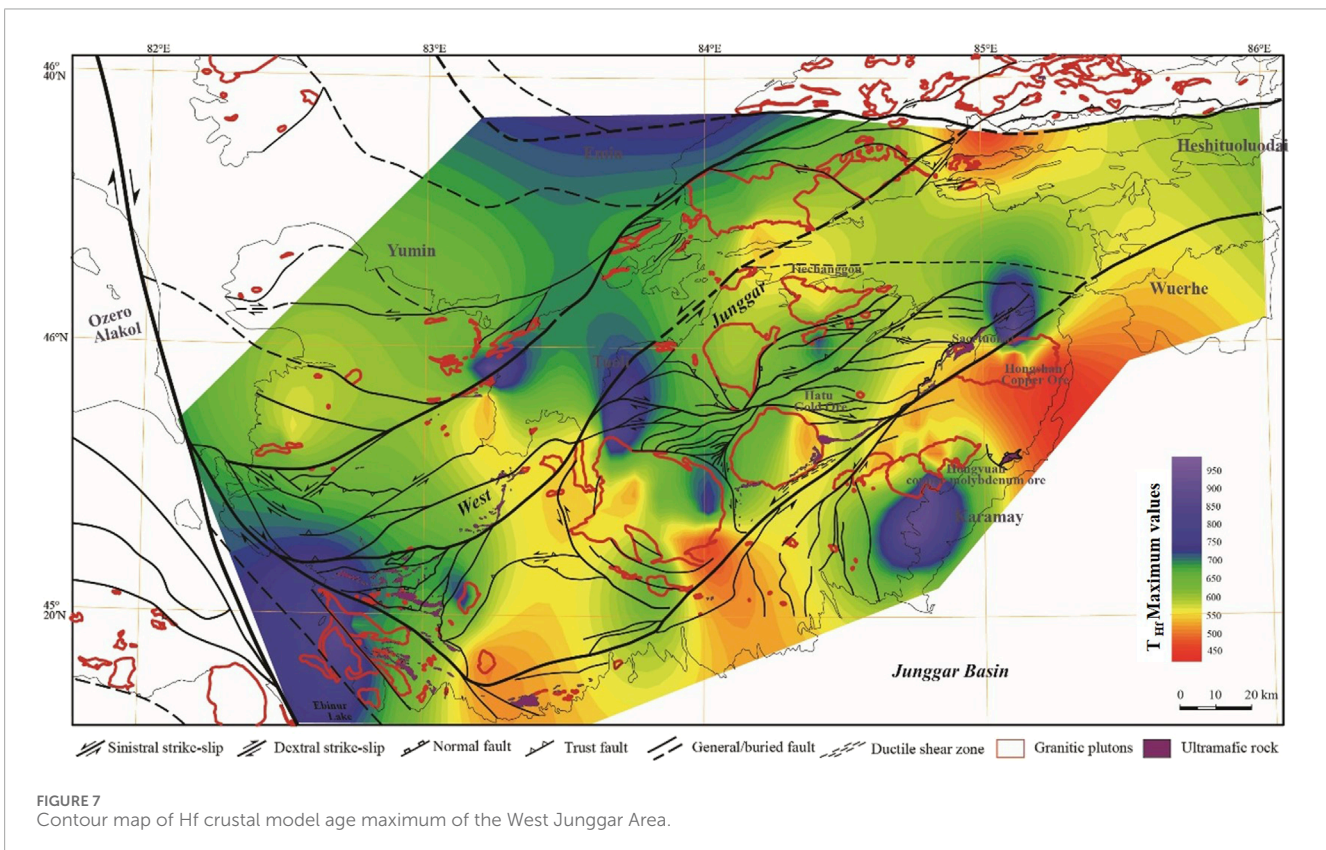
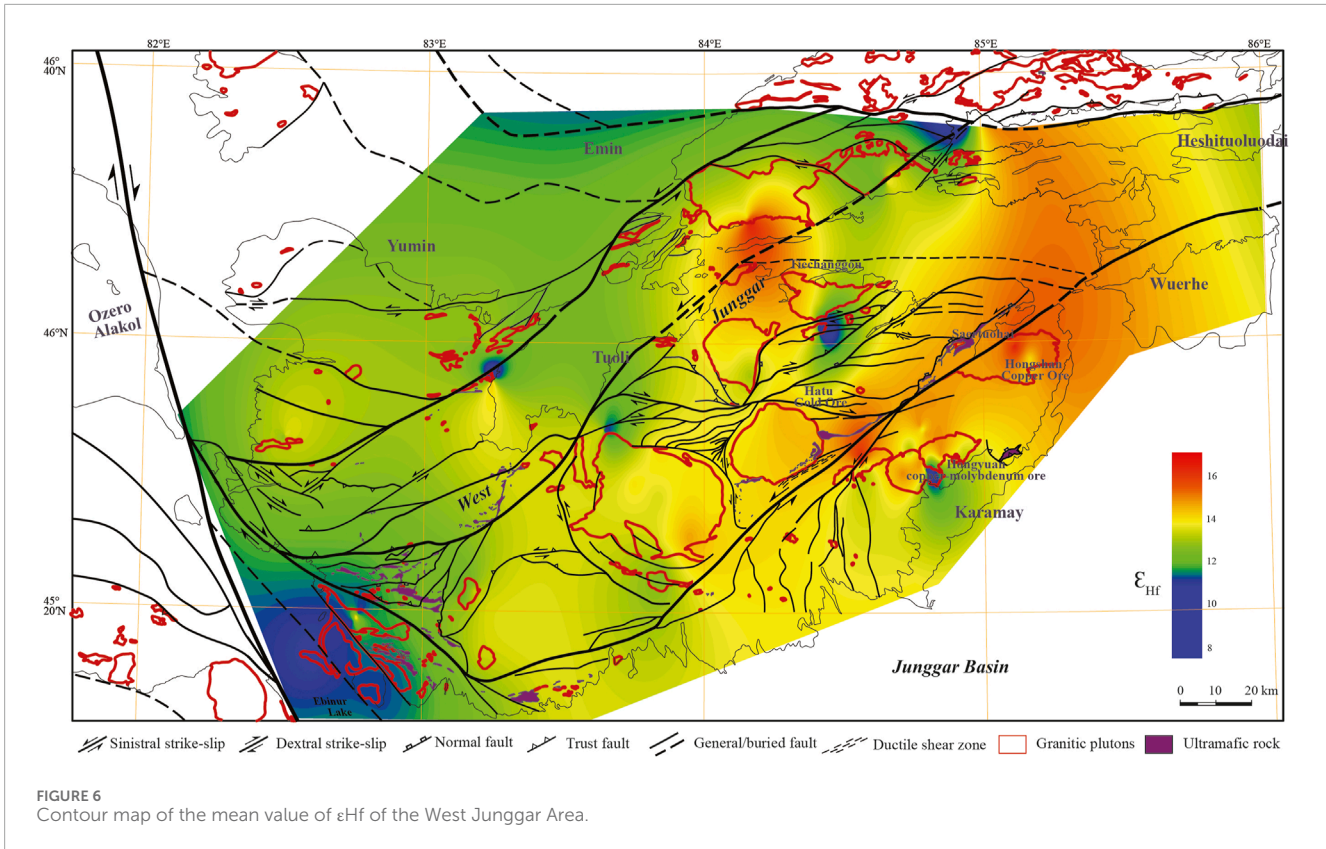
Geophysical exploration combined with surface geological surveys has been one of the most important means of probing the composition of the lithosphere. Xu et al. (2022a) concluded that there is a certain degree of correspondence between the aeromagnetic anomalous area and the isotope anomalous area, as evidenced by comparative analysis of regional aeromagnetic maps, gravity maps, and Sr-Nd-Pb contour maps. The Hf isotopic signatures of the rocks can indicate the properties of the deep source region. The Hf-Nd isotopic decoupling due to multiple factors can be excluded by calculating the average Hf isotope values and analyzing them compared to Nd isotopes. The whole-rock Sr-Nd-Pb isotope results of magma-mixed granites reflect the process of magma mixing, which cannot completely exclude the interference of ancient materials. Since Hf isotope values can be measured from single zircons and have a wide range of values in magmatic samples, it is possible to explore the presence of ancient material through Hf isotope signatures. The Sr-Nd-Pb isotope results generally indicate the absence of an ancient crystalline basement probably in the West Junggar region. To investigate the properties of the deep material source area, mean crustal model age maps were produced using

the Hf isotopes' arithmetic mean value and compared with the Nd isotope contour map. Additionally, the maximum value of the crustal model age map is produced using the minimum value of the Hf isotopes, which aids in the analysis of the composition of the deep ancient materials in the West Junggar area.

The age range of ancient crustal materials in the West Junggar area is extensive. (1) The maximum crustal model ages in some areas are about 400–550 Ma, which is near the Hongshan batholith, the Miaoergou batholith, and the Dulunhedong batholith near the Darabut fault, which indicates that the deep oldest crustal materials have been formed in the Early Paleozoic. (2) The maximum crustal model ages of large rock bases such as Miaoergou batholith, Hatu batholith, Tiechanggou batholith, Akbastao batholith, Hatu batholith, and Kurumus batholith are ~550–700 Ma, indicating that the deep oldest crustal material may have formed in the late Neoproterozoic. (3) The maximum crustal model ages in the southern part of Karamay, the northern part of Hongshan batholith, the southern and the western part of the Tuoli, and the Jietebudiao batholith is ~700–1,000 Ma, indicating that the oldest crustal material at depth may have formed in the Early Neoproterozoic (Figure 7).

In this paper, we produced a Pb-Nd-Hf isotope typical profile (The location of the profile is shown in Figure 2). To discuss the boundaries of the regional tectonics and the deep materials and the properties of the deep crust, we compared and analyzed the profile map between the magnetotelluric sounding (Xu et al., 2016), ( $^{206}\text{Pb}/^{204}\text{Pb}_i$ ), Hf crustal model maximum age and Nd model age comprehensively (Figure 8).

Although there are some differences in resistivity between the two sides of the Baerluk fault, Nd-Pb-Hf isotope values are



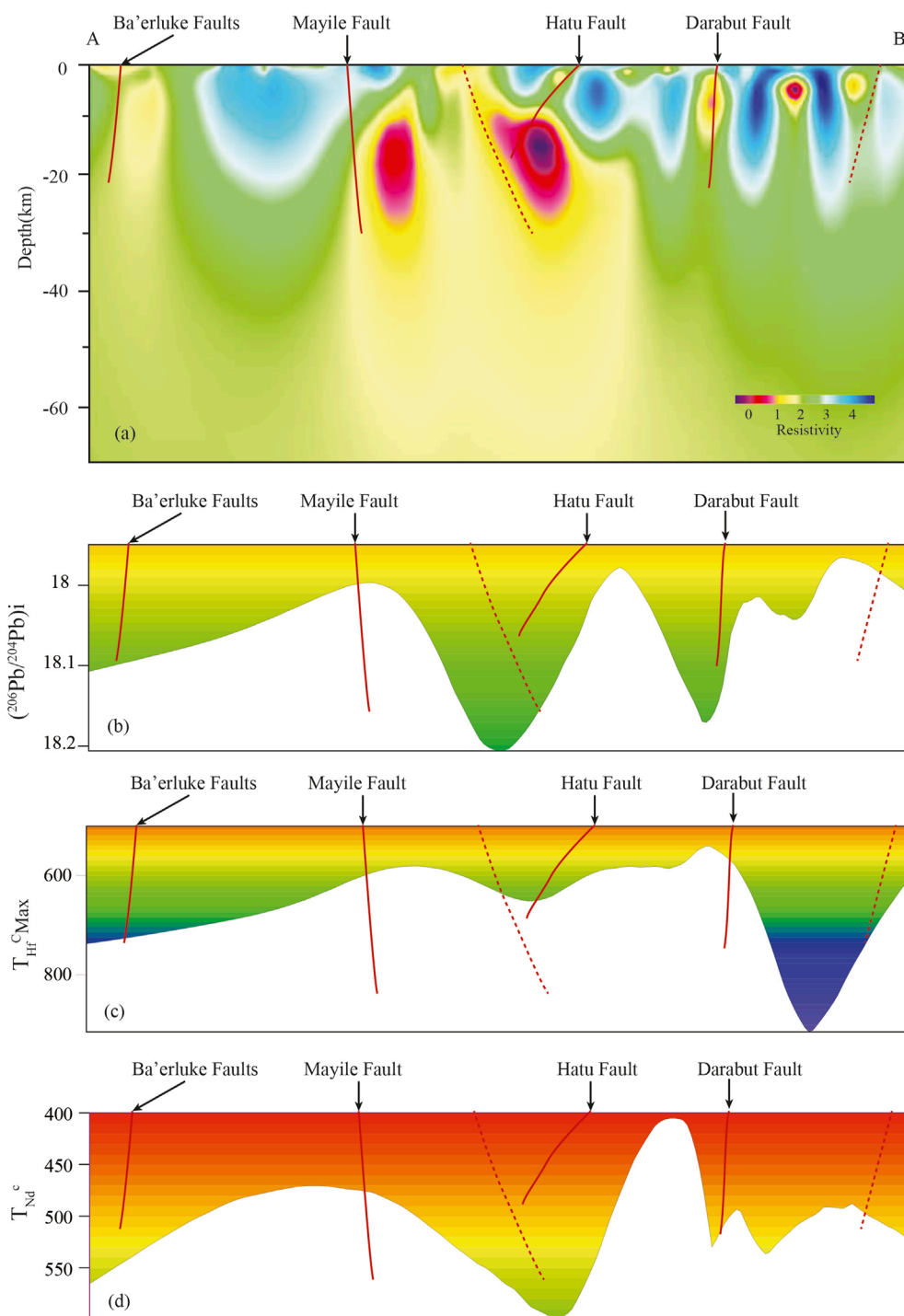


**FIGURE 8** Geological-geophysical-isotopic characterization of typical profiles of the West Junggar Area. (A) Magnetotelluric sounding profile (Xu et al., 2016), (B)  $(^{206}\text{Pb}/^{204}\text{Pb})_i$  profile, (C) Hf maximum mode age profile, (D) Nd model age profile. Profile location: (A) Ermin County, (B) Karamay City. (A, B) represents the location of the section in Figure 2.

more consistent, both indicating the age of deep crust material is relatively older. Near the Mayile Fault, the value of  $(^{206}\text{Pb}/^{204}\text{Pb})_i$  shows a decreasing trend, and the Nd-Hf mode age becomes younger, indicating that the age of deep material is gradually becoming younger.

In the region between the Mayile Fault and the Darabut Fault, the variations of Nd-Pb-Hf isotopic and the deep materials are relatively consistent, and have good correspondence. There are obvious electrical differences on both sides of the Darabut Fault, the Hatu Fault, and the Mayile Fault, which are also the inflection

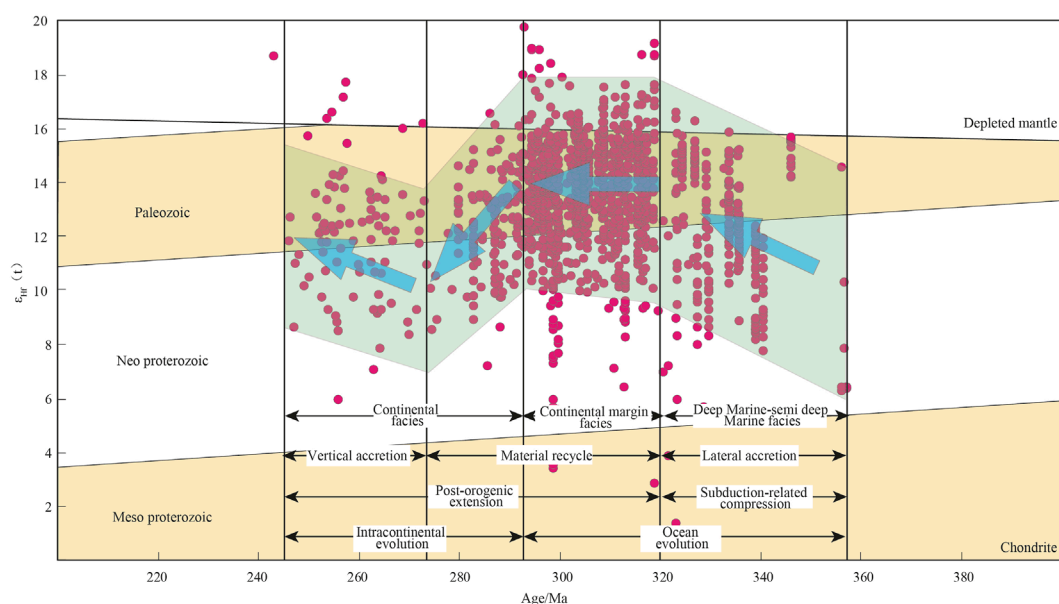


FIGURE 9  
Hf isotopic composition of Early Carboniferous-Early Triassic of the West Junggar Area.

points of Nd-Pb-Hf isotope changes. It can be concluded that there are highly comparable in some features of the geology, geophysics, and geochemistry of the West Junggar area through the above joint sections comparative study. It shows that the Isotopic mapping can provide sufficient evidence of deep material for the deep lithosphere study.

## 5.2 Deep material evolution

Previous studies have significant controversial on the crustal growth of the CAO/B during the Phanerozoic (Yang et al., 2017; Huang et al., 2018; Wang T. et al., 2018; Lv et al., 2017). Xu et al. (2022a) concluded that the mantle contribution values of West Junggar are all greater than 50%, concentrating on 75%–95% by performing Sr-Nd-Pb Isotopic mapping in the West Junggar area. It is indicated that the crustal growth volume of the West Junggar area is huge in the Late Paleozoic, the whole is greater than 50%.

In this paper, we map the scatter plot of Hf isotopes in the West Junggar area to discuss the evolution of deep crust during the Late Paleozoic (Figure 9). During the Early Carboniferous (~360–320 Ma), the Hf isotope values of the West Junggar area exhibited a gradual increase trend, indicating that the contribution degree of mantle source material to the crust is gradually increasing. During the Late Carboniferous-Early Permian (~320–294 Ma), in the West Junggar region, the Hf isotopic signature indicates that the predominant magmatism and the most significant crustal growth (the majority of the crustal growth volume was greater than 75%) due to the contribution of a considerable amount of mantle source material. Since the Early Permian (~294 Ma), there has been a notable decrease in the contribution of the juvenile mantle source material to the West Junggar region.

Although the isotopic values of intermediate-acid magmatism in the area still exhibit a relatively younger signature, the contribution of the juvenile material shows a gradual weakening trend compared with the previous peak of magmatism. During the Middle Permian to the Early Triassic, most regions of West Junggar experienced a quiescence period concerning hypogene magmatic activity, there were nevertheless significant deep magmatic intrusions in the southwestern Jietebudiao area (Xu et al., 2020). Furthermore, the contribution of juvenile material exhibits an upward trend.

## 5.3 Geotectonic evolution

The geotectonic evolution of the West Junggar area is controlled by the opening and closure of the Junggar Ocean closely. Existing evidence indicates that the primary evolutionary phase of the Junggar Ocean has been ongoing since the early Paleozoic.

Among them, the West Junggar Tangbala ophiolite mélanges (limited ocean basin) with the blueschist metamorphism (458–470 Ma; Zhang, 1997), the Hongguleleng ophiolite mélanges (Zhang and Huang, 1992; Zhang and Guo, 2010), and the Taerbahatai Kujibai ophiolite mélanges (Zhu and Xu, 2006) were formed in the Ordovician (He et al., 2007). The Karamay ophiolite mélanges may form in the Cambrian-Ordovician (He et al., 2007; Zhu et al., 2007). The Darabut ophiolite mélanges was formed in the Early Devonian (Feng et al., 1989; Zhang and Huang, 1992). These Early Paleozoic ophiolitic mélanges suggest that the West Junggar area was in the stage of oceanic basin evolution before the Early Carboniferous. So, the West Junggar area experienced the following four periods of tectonic evolution during the Late Paleozoic (Figure 10):

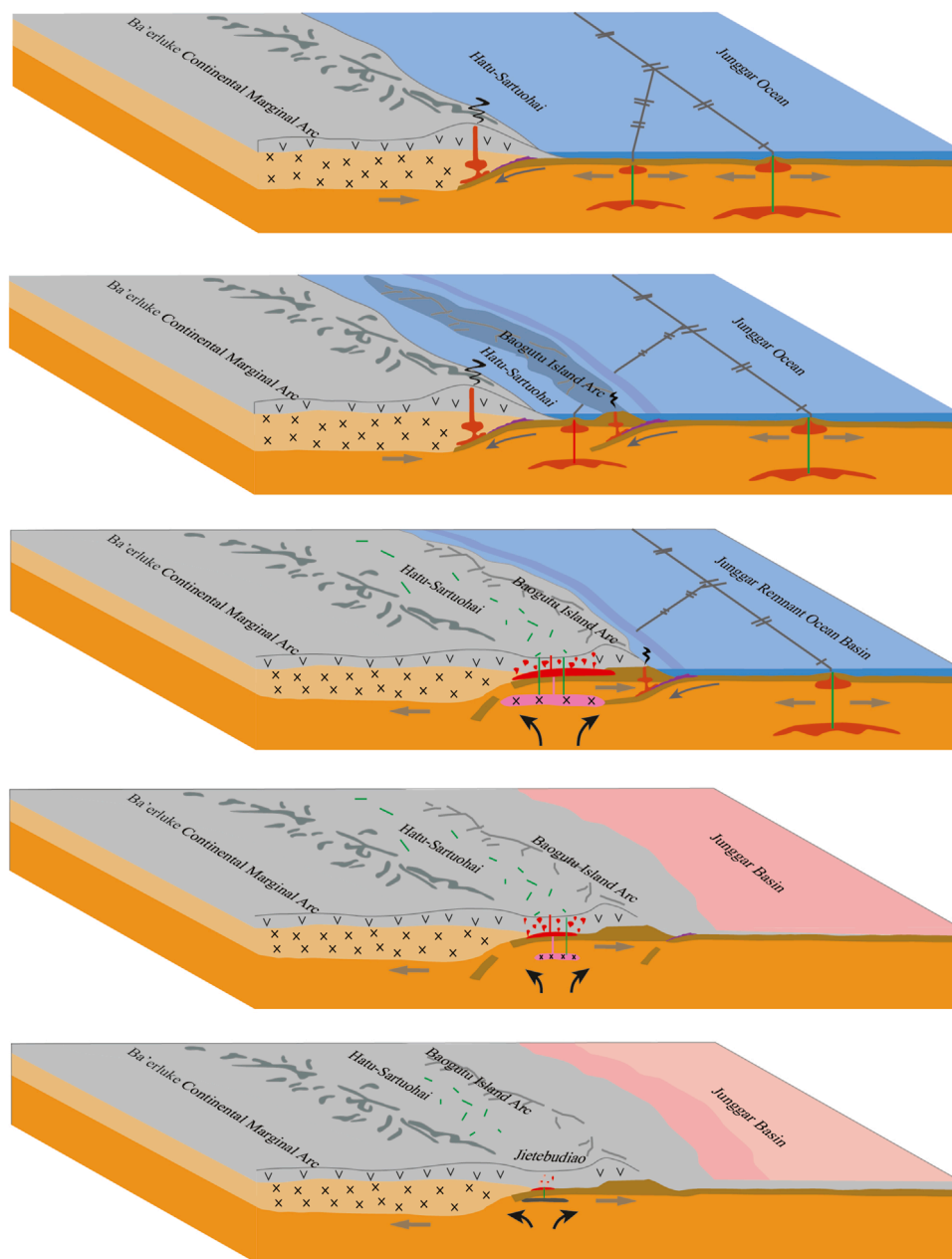


FIGURE 10 Carboniferous-Permian tectonic evolutionary pattern of the West Junggar Area.

- (1) The Early Carboniferous Period (360–320 Ma). The Junggar Ocean underwent intra-oceanic subduction (Yang et al., 2017) and formed an intra-oceanic arc represented by the Bogutu Island Arc (Tong et al., 2014), which is similar to the multi-oceanic island form of the West Pacific tectonic domain. The arc is dominated by I-type granitoids (including adakites) and deposits a set of huge deep-sea and semi-deep-sea sedimentary constructions (An and Zhu, 2009). A large amount of juvenile crust was continuously added under the oceanic crust and islands of the West Junggar area as the subduction progressed. The Hf isotopes overall exhibited a trend of gradual increase, and the crust underwent lateral accretion.
- (2) The Late Carboniferous–Early Permian Period (320–294 Ma). The West Junggar area completed the ocean-land tectonic transition as the weakened subduction gradually of the Junggar Ocean (Shi et al., 2017; Xu et al., 2019a; Ma et al., 2020). Under the post-orogenic extension of the tectonic background characterized by crustal stretching and thinning, lower pressure, and mantle magma upwelled. The lower and middle crust was molten by heat, and the extremely intense magmatism, a large granitic basement dominated by A-type granites was formed (Han et al., 2006; Huang et al., 2016; Chen et al., 2010). The I-type granite with characteristics of crust-mantle mixing was formed by the mixing between basite

formed by the lower-middle crust and acidic magma chamber. Some of these contributed to the growth crust of the Western Junggar region in the form of the intermediate-basic dike along the tensile fissure (Xu et al., 2022b; Duan et al., 2021). The sedimentary construction has transitioned from deep-sea to semi-deep-sea facies evolved into continental slope facies in the West Junggar area as the extension ongoing, the crust thickened, and seawater receded (He et al., 2004; Ji and Li, 1998). In general, the Late Carboniferous-Early Permian was the most intense period of magmatism in the West Junggar area. The crustal growth may have been dominated by the recirculation of Paleoproterozoic oceanic crust or oceanic island arcs, or with a small amount of juvenile material formed directly by mantle magmatism during the basement intrusion, and the crustal growth volume may have been as high as 75% or more in most areas.

- (3) The Early Permian Period (294–272 Ma). The magmatic activity in the West Junggar area was weakened, and the contribution of juvenile materials showed a gradual weakening trend compared with the previous peak period of magmatic activity (Yin et al., 2011). The emergence of the red mullite assemblage (Zhu et al., 2013) indicated that the West Junggar area was already in the intra-terrestrial evolution stage.
- (4) The Early Permian-Early Triassic Period (272–250 Ma). The deep magmatic intrusion observed in most areas of the West Junggar had largely finished, except in the southwestern region, where the Jietebudiao batholith was still undergoing multiple phases of deep magmatic intrusion (Xu et al., 2020). Under a high-temperature, low-pressure, crustal-thinning extensional environment, in the Jietebudiao area, the upwelling of mantle magmas brought a considerable amount of heat and juvenile materials, resulting in the formation of shell-mantle mixed-source I-type granites and highly differentiated I-type granites, in which the crust is predominantly vertically accretionary. Most areas of West Junggar in a weather and denudation intracontinental setting controlled by the Continued crustal uplift during the Middle and Late Permian, which resulted in the absence of the Middle and Upper Permian.

## 6 Conclusion

- (1) Whole-rock Sr-Nd-Pb-Hf Isotopic mapping studies indicate that the deep material in the West Junggar area is dominated by the Paleozoic juvenile crust, with a limited ancient crystalline basement.
- (2) The West Junggar area is characterized by higher positive  $\epsilon_{\text{Hf}}(t)$ , higher positive  $\epsilon_{\text{Nd}}(t)$ , lower  $(^{87}\text{Sr}/^{86}\text{Sr})_i$ , and young crustal model ages. During the Late Paleozoic Carboniferous-Permian, ~85% of the area of West Junggar had a crustal growth volume of 75%–95%, which was dominated by lateral crustal growth and material recirculation. ~15% of the area (the Jietebudiao area) had a crustal growth volume of 50%–75%, which was dominated by vertical crustal growth.
- (3) The West Junggar area experienced the multistage evolution during the Late Paleozoic: The Early Carboniferous was

characterized by intra-oceanic subduction with the juvenile material constantly contributing to the lateral accretion of the crust. During the post-orogenic extension stage in Late Carboniferous - Early Permian, the magmatism was concentrated during this period and the huge amount of juvenile mantle source mixed, and the crustal growth volume may be as high as 75% or more. In the Early Permian, the region entered the intracontinental evolution stage, magmatic activity weakened, and the involvement of juvenile material gradually decreased. During the Middle Permian-Early Triassic, the southwestern Jietebudiao region remains the magmatism activity and resulting in the increased amount of juvenile material contributed to the crust growth.

## Data availability statement

The original contributions presented in the study are included in the article/[Supplementary Material](#), further inquiries can be directed to the corresponding authors.

## Author contributions

SX: Conceptualization, Data curation, Formal Analysis, Investigation, Methodology, Project administration, Resources, Supervision, Validation, Visualization, Writing–original draft, Writing–review and editing. WD: Conceptualization, Data curation, Formal Analysis, Investigation, Project administration, Software, Supervision, Visualization, Writing–review and editing. FM: Formal Analysis, Investigation, Writing–review and editing. XC: Conceptualization, Formal Analysis, Funding acquisition, Data curation, Writing–original draft, Investigation, Methodology. ZS: Data curation, Funding acquisition, Investigation, Writing–review and editing. LH: Software, Visualization, Writing–review and editing. PH: Data curation, Investigation, Writing–original draft. JS: Investigation, Software, Writing–original draft. XY: Software, Writing–review and editing.

## Funding

The author(s) declare that financial support was received for the research, authorship, and/or publication of this article. This study was financially supported by the China National Science and Technology Major Project (2024ZD1001106), the China Geological Survey (DD20230008, DD20230229, DD20160083) and the Fundamental Research Funds for the Chinese Academy of Geological Sciences (JKY202011).

## Acknowledgments

We thank the members of the Deep Geology Department of the Chinese Academy of Geological Sciences for their assistance.

## Conflict of interest

The authors declare that the research was conducted in the absence of any commercial or financial relationships that could be construed as a potential conflict of interest.

## Publisher's note

All claims expressed in this article are solely those of the authors and do not necessarily represent those of their affiliated

organizations, or those of the publisher, the editors and the reviewers. Any product that may be evaluated in this article, or claim that may be made by its manufacturer, is not guaranteed or endorsed by the publisher.

## Supplementary material

The Supplementary Material for this article can be found online at: <https://www.frontiersin.org/articles/10.3389/feart.2025.1465894/full#supplementary-material>

## References

- An, F., and Zhu, Y. F. (2009). SHRIMP U-Pb zircon ages of tuff in Baogutu Formation and their geological significances. *Acta Petrol. Sin.* 25 (6), 1437–1445.
- Bao, Z., Chen, L., Zong, C., Yuan, H. L., Chen, K. Y., and Dai, M. (2017). Development of pressed sulfide powder tablets for, *in situ*, sulfur and lead isotope measurement using LA-MC-ICP-MS. *Int. J. Mass. Spectrom.* 421, 255–262. doi:10.1016/j.ijms.2017.07.015
- Buslov, M., Fujiwara, Y., Iwata, K., and Semakov, N. (2004). Late paleozoic-early mesozoic geodynamics of central asia. *Gondwana Res.* 7 (3), 791–808. doi:10.1016/S1342-937X(05)71064-9
- Chen, H. H., Li, X., and Ding, X. W. (2007). Twelve kinds of gridding methods of Surfer8.0 in isoline drawing. *J. Eng. Geophys.* 4 (1), 52–57.
- Chen, J. F., Han, B. F., Ji, J. Q., Zhang, L., Xu, Z., He, G. Q., et al. (2010). Zircon U-Pb ages and tectonic implications of paleozoic plutons in northern West Junggar, north xinjiang, China. *Lithos* 115, 137–152. doi:10.1016/j.lithos.2009.11.014
- Chen, J. F., Han, B. F., Zhang, L., Xu, Z., Liu, J. L., Qu, W. J., et al. (2015a). Middle paleozoic initial amalgamation and crustal growth in the west junggar (nw China): constraints from geochronology, geochemistry and Sr–Nd–Hf–Os isotopes of calc-alkaline and alkaline intrusions in the xiemisitai-saier mountains. *J. Asian Earth Sci.* 113, 90–109. doi:10.1016/j.jseas.2014.11.028
- Chen, S. S., Su, X. P., Zheng, J. P., and Wei, Y. (2013b). Geochemical characteristics of Karamay Jurassic basalts and implication on crust-mantle interaction. *Chem. Geol.* 42 (1), 29–45.
- Chen, X. H., Chen, Z. L., Bai, Y. F., Han, S. Q., Ding, W. C., Li, J. Y., et al. (2016). Late Paleozoic concentrated mineralization of balkhash-junggar metallogenic belt in the western part of the central asia metallogenic domain. *J. Earth Sci. Environ.* 38 (3), 285–305. doi:10.3969/j.issn.1672-6561.2016.03.001
- Chen, X. H., Chen, Z. L., Han, S. Q., Wang, Z. H., Yang, Y., Ye, B. Y., et al. (2013a). Late Paleozoic magmatic and porphyry copper metallogenesis in Balkhash metallogenic Zone. *Cent. Asia. J. Jilin Univ. Earth Sci.* 43 (3), 734–747.
- Chen, X. H., Chen, Z. L., Han, S. Q., Wang, Z. H., Yang, Y., Ye, B. Y., et al. (2012b). Geothermochronology of Mo-W deposits in balkhash metallogenic belt, Kazakhstan, central asia. *Earth Sci.* 37 (5), 878–892. doi:10.3799/dqkx.2012.097
- Chen, X. H., Chen, Z. L., Han, S. Q., Yang, Y., Wang, Z. H., Jia, M. X., et al. (2017). *Tectonic-magmatic-mineralization evolution in Balkhash-West Junggar and adjacent areas*. Beijing: Science Press, 71–83.
- Chen, X. H., Chen, Z. L., and Yang, N. (2009). Study on regional mineralization and ore-field structures: building of mineralizing tectonic systems. *J. Geomechanics* 15 (1), 1–19. doi:10.3969/j.issn.1006-6616.2009.01.001
- Chen, X. H., Dong, S. W., Shi, W., Ding, W. C., Zhang, Y. P., Li, B., et al. (2022). Construction of the continental asia in phanerozoic: a review. *Acta Geol. Sin-Engl* 96 (1), 26–51. doi:10.1111/1755-6724.14867
- Chen, X. H., Seitmuratova, E., Wang, Z. H., Chen, Z. L., Han, S. Q., Li, Y., et al. (2014). SHRIMP U-Pb and Ar-Ar geochronology of major porphyry and skarn Cu deposits in the Balkhash Metallogenic Belt, Central Asia, and geological implications. *J. Asian Earth Sci.* 79 (2), 723–740. doi:10.1016/j.jseas.2013.06.011
- Chen, X. H., Wang, Z. H., Chen, Z. L., Han, S. Q., Seitmuratova, E., Yang, Y., et al. (2012a). Geochronological constraints on skarn copper metallogenesis of the large-scale Sayak ore field, Kazakhstan, Central Asia. *Acta Petrol. Sin.* 28 (7), 1981–1994.
- Chen, X. H., Wang, Z. H., Chen, Z. L., Seitmuratova, E., Han, S. Q., Zhou, Q., et al. (2015b). SHRIMP U-Pb, Ar-Ar and fission-track geochronology of W-Mo deposits in the Balkhash Metallogenic Belt (Kazakhstan): central Asia, and the geological implications. *J. Asian Earth Sci.* 110 (2), 19–32. doi:10.1016/j.jseas.2014.07.016
- Chen, X. H., Yang, N., Ye, B. Y., Wang, Z. H., and Chen, Z. L. (2011). Tectonic system and its control on metallogenesis in West Junggar as part of the central asia multi-core metallogenic system. *Geotecton. Metallog.* 35 (3), 325–338. doi:10.3969/j.issn.1001-1552.2011.03.001
- Ding, W. C., Li, T. D., Chen, X. H., Chen, J. P., Xu, S. L., Zhang, Y. P., et al. (2020). Intra-continental deformation and tectonic evolution of the West Junggar Orogenic Belt, Central Asia: evidence from remote sensing and structural geological analyses. *Geosci. Front.* 11 (2), 651–663. doi:10.1016/j.gsf.2019.08.001
- Duan, F. H., Zhi, Q., Li, Y. J., Xiao, H., Wang, P. L., and Gao, J. P. (2021). Petrogenesis and geodynamic setting of the Late Carboniferous granodiorite porphyry in Miaogou pluton, southern West Junggar. *Acta Petrol. Sin.* 37 (4), 1159–1176. doi:10.18654/1000-0569/2021.04.12
- Feng, Y., Coleman, R., Tilton, G., and Xiao, X. (1989). Tectonic evolution of the West junggar region, xinjiang, China. *Tectonics* 8 (4), 729–752. doi:10.1029/TC008i004p00729
- Geng, H. Y., Sun, M., Yuan, C., Xiao, W. J., Xian, W. S., Zhao, G. C., et al. (2009). Geochemical, Sr–Nd and zircon U–Pb–Hf isotopic studies of late carboniferous magmatism in the West junggar, xinjiang: implications for ridge subduction. *Chem. Geol.* 266 (3–4), 364–389. doi:10.1016/j.chemgeo.2009.07.001
- Han, B. F., He, G. Q., Wang, S. G., and Hong, D. W. (1998). Postcollisional mantle-derived magmatism and vertical growth of the continental crust in North Xinjiang. *Geol. Rev.* 44 (4), 396–404.
- Han, B. F., Ji, J. Q., Song, B., Chen, L. H., and Zhang, L. (2006). Late Paleozoic vertical growth of continental crust around the Junggar Basin, Xinjiang, China (Part I): timing of post-collisional plutonism. *Acta Petrol. Sin.* 22 (5), 1077–1086.
- Han, L. L., Ding, W. C., Chen, X. H., Liu, M. L., Wang, Y., Xu, S. L., et al. (2019). Linear structure extraction and quantitative analysis of multi-source remote sensing information in West Junggar Basin. *China Geol.* 46 (5), 1209–1223. doi:10.12029/gc20190501
- He, G. Q., Cheng, S. D., Xu, X., Li, J. X., and Hao, J. (2004). *Geotectonic map of Xinjiang and adjacent areas of China (1:2500000, with instructions)*. Beijing: Science Press, 1–65.
- He, G. Q., Liu, J. B., Zhang, Y. Q., and Xu, X. (2007). Karamay ophiolitic mélange formed during Early Paleozoic in western Junggar basin. *Acta Petrol. Sin.* 23 (7), 1573–1576.
- Hou, Z. Q., and Wang, T. (2018). Isotopic mapping and deep material probing (II): imaging crustal architecture and its control on mineral systems. *Geosci. Front.* 25 (6), 20–41. doi:10.13745/j.esf.sf.2018.11.19
- Huang, H., Wang, T., Zhang, Z. C., Li, C., and Qin, Q. (2018). Highly differentiated fluorine-rich, alkaline granitic magma linked to rare metal mineralization: a case study from the Boziguoèr rare metal granitic pluton in South Tianshan Terrane, Xinjiang, NW China. *Ore Geol. Rev.* 96, 146–163. doi:10.1016/j.oregeorev.2018.04.021
- Huang, P. H., Chen, X. H., Wang, Z. H., Ye, B. Y., Li, Z. X., and Yang, Y. (2016). Late Paleozoic granitic magmatism in western Junggar metallogenic belt (Xinjiang), Central Asian, and its tectonic implication. *Geotecton. Metallog.* 40 (01), 145–160. doi:10.16539/j.ddgzycckx.2016.01.013
- Jahn, B. M. (2004). The central asian orogenic belt and growth of the continental crust in the phanerozoic. *Geol. Soc. Lond. Spec. Publ.* 226 (1), 73–100. doi:10.1144/GSL.SP.2004.226.01.05
- Jiang, Y., Xiao, L., Zhou, P., and Wang, G. C. (2015). Geological, geochemical characteristics of hongshan pluton: constraint for lower crust of West Junggar, xinjiang. *Earth Sci. Wuhan. China* 40 (7), 1129–1147. doi:10.3799/dqkx.2015.095
- Jin, H. J., and Li, Y. C. (1998). Study on the sedimentary structure of Carboniferous biogenic in the northwestern margin of Junggar Basin. *Geol. Bull. China* 43 (17), 1888–1891.
- Jin, S., Rong, G. L., Zhang, Z. Y., Li, T. G., Peng, C. H., and Wu, L. A. (2016). Geochemical characteristics and zircon U–Pb age of the kuoitais complex in the mayile mountains of West Junggar in xinjiang. *China Geol.* 43 (1), 99–110. doi:10.3969/j.issn.1000-3657.2016.01.007

- Li, D., He, D., and Fan, C. (2015). Geochronology and Sr-Nd-Hf isotopic composition of the granites, enclaves, and dikes in the Karamay area, NW China: insights into late Carboniferous crustal growth of West Junggar. *Geosci. Front.* 6 (2), 153–173. doi:10.1016/j.gsf.2013.10.005
- Li, D., He, D. F., Yang, Y. H., and Lian, Y. C. (2014). Petrogenesis of mid-Carboniferous volcanics and granitic intrusions from western Junggar Basin boreholes: geodynamic implications for the Central Asian Orogenic Belt in Northwest China. *Int. Geol. Rev.* 56 (13), 1668–1690. doi:10.1080/00206814.2014.958766
- Li, H., Sun, H. S., Wu, J. H., Evans, N. J., Xi, X. S., Peng, N. L., et al. (2017). Re–Os and U–Pb geochronology of the Shazigou Mo polymetallic ore field, Inner Mongolia: implications for Permian–Triassic mineralization at the northern margin of the North China Craton. *Ore Geol. Rev.* 83, 287–299. doi:10.1016/j.oregeorev.2016.12.010
- Liu, B., Hou, L. X., Xu, Y., Ju, N., Ma, J. X., Xie, Z. H., et al. (2023). Zircon U–Pb–Hf isotopes and whole-rock geochemistry of the “kulumudi formation” from the laofengkou area (West Junggar): implications of the construction of a juvenile arc in the junggar–balkhash ocean. *Minerals* 14 (1), 14. doi:10.3390/min14010014
- Liu, C., and Nie, F. (2015). Permian magmatic sequences of the Bilihe gold deposit in central Inner Mongolia, China: petrogenesis and tectonic significance. *Lithos* 231, 35–52. doi:10.1016/j.lithos.2015.06.010
- Lkhagvasuren, D. O., Oyunchimeg, T. U., Enkhdalai, B., Safonova, I., Li, H., Otgonbaatar, D., et al. (2020). Middle Paleozoic intermediate-mafic rocks of the Tsoroidog Uul’ accretionary complex, Central Mongolia: petrogenesis and tectonic implications. *Lithos* 376–377, 105795. doi:10.1016/j.lithos.2020.105795
- lv, B., Wang, T., Tong, Y., Zhang, L., Yang, Q. D., and Zhang, J. J. (2017). Spatial and temporal distribution and tectonic settings of magmatic-hydrothermal ore deposits in the Eastern Central Asia Orogen Belt. *J. Jilin Univ. Earth Sci. Ed.* 47 (2), 305–343. doi:10.13278/j.cnki.jjuese.201702101
- Ma, F. Z., Chen, X. H., Xu, S. L., Ma, F., Han, L. L., Ding, W. C., et al. (2020). LA–ICP–MS zircon U–Pb dating and geochemistry of Late Paleozoic sanukitoids in Hongshan area, West Junggar. *Acta Geol. Sin.* 94 (05), 1462–1481. doi:10.19762/j.cnki.dizhixuebao.2020140
- Shen, P., Pan, H. D., Cao, C., Zhong, S. H., and Li, C. H. (2017). The formation of the Suyunhe large porphyry Mo deposit in the West Junggar terrain, NW China: zircon U–Pb age, geochemistry and Sr–Nd–Hf isotopic results. *Ore Geol. Rev.* 81 (2), 808–828. doi:10.1016/j.oregeorev.2016.02.015
- Shen, P., Shen, Y. C., Liu, T. B., Zhang, R., Wang, J. B., Zhang, Y. X., et al. (2009). Host rocks and alteration characters of the Baogutu porphyry Copper-molybdenum deposit in Xinjiang, NW China. *Acta Petrol. Sin.* 25 (4), 777–792. doi:10.1111/1467-8462.00293
- Shen, P., Zhou, T. F., Yuan, F., Pan, H. D., Wang, J. L., and Seitmuratova, E. (2015). Main deposit types, mineral systems, and metallogenic belt connections in the Circum-Balkhash–West Junggar metallogenic province. *Acta Petrol. Sin.* 31 (2), 285–303.
- Shi, J. J., Chen, X. H., Ding, W. C., and Li, B. (2017). Late Paleozoic ocean-continent transition in West Junggar, central asia orogenic belt: evidence from late carboniferous rhyolites. 23(1), 150–160.
- Su, Y. P., Tang, H. F., Hou, G. S., and Liu, C. Q. (2006). Geochemistry of aluminous A-type granites along Darabut tectonic belt in West Junggar, xinjiang. *Chem. Geol.* 35 (1), 55–67. doi:10.3321/j.issn:0379-1726.2006.01.007
- Sun, H. S., Li, H., Danišik, M., Xia, Q. L., Jiang, C. L., Wu, P., et al. (2017). U–Pb and Re–Os geochronology and geochemistry of the Donggebi Mo deposit, Eastern Tianshan, NW China: insights into mineralization and tectonic setting. *Ore Geol. Rev.* 86, 584–599. doi:10.1016/j.oregeorev.2017.03.020
- Tang, G., Wang, Q., Wyman, D., Li, Z. X., Xu, Y. G., and Zhao, Z. H. (2012). Recycling oceanic crust for continental crustal growth: Sr–Nd–Hf isotope evidence from granitoids in the western Junggar region, NW China. *Lithos* 128–131, 73–83. doi:10.1016/j.lithos.2011.11.003
- Tang, G., Wang, Q., Wyman, D., Li, Z. X., Zhao, Z. H., Jia, X. H., et al. (2010a). Ridge subduction and crustal growth in the Central Asian Orogenic Belt: evidence from Late Carboniferous adakites and high-Mg diorites in the western Junggar region, northern Xinjiang (west China). *Chem. Geol.* 277 (3), 281–300. doi:10.1016/j.chemgeo.2010.08.012
- Tang, G., Wang, Q., Wyman, D., Sun, M., Li, Z. X., Zhao, Z. H., et al. (2010b). Geochronology and geochemistry of Late Paleozoic magmatic rocks in the Lamasu–Dabate area, northwestern Tianshan (west China): evidence for a tectonic transition from arc to post-collisional setting. *Lithos* 119 (3–4), 393–411. doi:10.1016/j.lithos.2010.07.010
- Tang, G. J., Wang, Q., Zhao, Z. H., Wyman, D. A., Chen, H. H., Jia, X. H., et al. (2009). Geochronology and geochemistry of the Ore-bearing porphyries in the Baogutu Area (West Junggar): petrogenesis and their implications for tectonics and Cu–Au mineralization. *J. Jilin Univ. Earth Sci.* 34 (1), 56–74. doi:10.3321/j.issn:1000-2383.2009.01.007
- Tian, Y. Z., and Yang, J. S. (2015). The genesis of peridotite in Darbute ophiolite within West Junggar basin, Xinjiang. *China Geol.* 42 (5), 1379–1403. doi:10.3969/j.issn.1000-3657.2015.05.014
- Tong, L. Y., Li, Y. J., Tian, R., Zhang, H. W., Wang, N. J., and Wang, R. (2014). Geochemical characteristics and tectonic significance of Carboniferous Baogutu Formation volcanic rocks in western Junggar, Xinjiang. *Xinjiang Geol.* 32 (2), 147–152.
- Wang, M., Wang, J. L., Hu, Y., and Wang, J. Q. (2017). Geochemistry, geochronology, whole rock Sr–Nd and zircon Hf isotopes of the Wulansala granite pluton in Xiemisitai area, Xinjiang. *Acta Petrol. Sin.* 34 (3), 618–636.
- Wang, T., and Hou, Z. Q. (2018). Isotopic mapping and deep material probing(I): revealing the compositional evolution of the lithosphere and crustal growth processes. *Geosci. Front.* 25 (6), 1–19. doi:10.13745/j.esf.2018.11.21
- Wang, X. S., Cai, K. D., Sun, M., Xiao, W. J., Xia, X., Wan, B., et al. (2018a). Two contrasting Late Paleozoic magmatic episodes in the northwestern Chinese Tianshan Belt, NW China: implication for tectonic transition from plate convergence to intra-plate adjustment during accretionary orogenesis. *J. Asian Earth Sci.* 153 (2), 118–138. doi:10.1016/j.jseas.2017.03.013
- Wang, T., Tong, Y., Wang, X., Mao, J. R., Zhang, H. R., Huang, H., et al. (2018b). Some progress on understanding the Phanerozoic granitoids in China. *China Geol.* 1 (1), 84–108. doi:10.31035/cg2018010
- Wu, C., Hong, T., Xu, X. W., Cao, M. J., Li, H., Zhang, G. L., et al. (2018). Tectonic evolution of the paleozoic barluk continental arc, West Junggar, NW China. *J. Asian Earth Sci.* 160, 48–66. doi:10.1016/j.jseas.2018.04.008
- Wu, J. H., Li, H., Xi, X. S., Kong, H., Wu, Q. H., Peng, N. L., et al. (2017). Geochemistry and geochronology of the mafic dikes in the taipusi area, northern margin of north China Craton: implications for silurian tectonic evolution of the central asian orogen. *J. Earth Syst. Sci.* 126, 64. doi:10.1007/s12040-017-0841-z
- Xiao, W. J., Li, S. Z., Santosh, M., and Jahn, B. (2012). Orogenic belts in central asia: correlations and connections. *J. Asian Earth Sci.* 49 (3), 1–6. doi:10.1016/j.jseas.2012.03.001
- Xiao, W. J., Shu, L. S., Gao, J., Xiong, X. L., Wang, J. B., Guo, Z. J., et al. (2008). Geodynamic processes of the central asia orogenic belt and its metallogeny. *Xinjiang Geol.* 26 (1), 4–8. doi:10.3969/j.issn.1000-8845.2008.01.002
- Xu, S. L., Chen, X. H., Li, T. D., Ding, W. C., Li, B., Zhang, Y. Y., et al. (2020). The latest magma intrusion activities in the west Junggar: constraints from the Early Permian–Early Triassic Jietebudiao pluton. *Acta Geol. Sin.* 94 (4), 1067–1090. doi:10.19762/j.cnki.dizhixuebao.2020001
- Xu, S. L., Chen, X. H., Li, T. D., Ding, W. C., Shi, J. J., Li, B., et al. (2019a). Time of the ocean-continent transition in West Junggar: constraints from zircon U–Pb dating and Lu–Hf isotopic composition. *China Geol.* 46 (5), 1061–1078. doi:10.12029/gc20190508
- Xu, S. L., Chen, X. H., Li, T. D., Shi, J. J., Ding, W. C., Li, B., et al. (2019b). The late carboniferous–early permian ocean-continent transition in the West junggar, central asian orogenic belt: constraints from columnar jointed rhyolite. *Acta Geol. Sin–Engl* 93 (2), 265–282. doi:10.1111/1755-6724.13812
- Xu, S. L., Ding, W. C., Chen, X. H., Li, T. D., Han, L. L., Liu, Y., et al. (2022a). Late Paleozoic crustal composition and growth in West Junggar: evidence from Sr–Nd–Pb isotopic mapping. *Geosci. Front.* 29 (2), 261–280. doi:10.13745/j.esf.2022.2.8
- Xu, S. L., Chen, X. H., Ma, F. Z., Shao, Z. G., Ding, W. C., Han, L. L., et al. (2022b). Petrogenesis of laba plutons in West Junggar, central asia orogenic belt: evidence from petrology, chronology, and geochemistry. *Acta Petrol. Sin.* 43 (6), 875–894. doi:10.3975/cagsb.2022.052601
- Xu, Y., Yang, B., Zhang, S., Liu, Y., Zhu, L. P., Huang, R., et al. (2016). Magnetotelluric imaging of a fossil paleozoic intraoceanic subduction zone in western Junggar, NW China. *J. Geophys. Res. Solid Earth* 121 (6), 4103–4117. doi:10.1002/2015JB012394
- Yang, F., Leng, C. B., Shen, X. M., Bagas, L., Zhang, L., and Jepsen, G. (2024). Editorial: evolution of tectonic structures and mineralisation in orogens and their margins. *Front. Earth Sci.* 12, 1371835. doi:10.3389/feart.2024.1371835
- Yang, F., Li, J. Z., Lu, S., Bian, B. L., Liu, H. L., Wei, Y. Z., et al. (2023). Carboniferous to early permian tectono-sedimentary evolution in the western junggar basin, NW China: implication for the evolution of Junggar Ocean. *Front. Earth Sci.* 11, 1237367. doi:10.3389/feart.2023.1237367
- Yang, G., Xiao, L., Wang, G. C., Gao, R., He, X. X., Zhang, L. C., et al. (2015). Geochronological, geochemical and petrogenesis of Bieluagaxi granodioritic pluton in West Junggar. *J. Jilin Univ. Earth Sci.* 40 (5), 810–823. doi:10.3799/dqkx.2015.066
- Yang, Q., Wang, T., Guo, L., Tong, Y., Zhang, L., Hou, Z. Q., et al. (2017). Nd isotopic variation of Paleozoic–Mesozoic granitoids from the Da Hinggan Mountains and adjacent areas, NE Asia: implications for the architecture and growth of continental crust. *Lithos* 272–273, 164–184. doi:10.1016/j.lithos.2016.11.015
- Yin, J. Y., Chen, W., Yu, S., Sun, J. B., Zhang, B., Yang, L., et al. (2016). Geochemical characteristics of early permian quartz syenite porphyry from northern West Junggar and their tectonic implication. *Acta Geol. Sin.* 90 (9), 2355–2364. doi:10.3969/j.issn.0001-5717.2016.09.016
- Yin, J. Y., Chen, W., Yuan, C., Yu, S., Xiao, W. J., Long, X. P., et al. (2015). Petrogenesis of early carboniferous adakitic dikes, sawur region, northern West Junggar, NW China: implications for geodynamic evolution. *Gondwana Res.* 27 (4), 1630–1645. doi:10.1016/j.gr.2014.01.016
- Yin, J. Y., Yuan, C., Wang, Y. J., Long, X. P., and Guan, Y. L. (2011). Magmatic records on the Late Paleozoic tectonic evolution of West Junggar, xinjiang. *Geotecton. Metallog.* 35 (2), 278–291. doi:10.16539/j.ddgzyckx.2011.02.013
- Yuan, H., Gao, S., Dai, M., Zong, C. L., Günther, D., Fontaine, G. H., et al. (2008). Simultaneous determinations of U–Pb age, Hf isotopes and trace element compositions

- of zircon by excimer laser-ablation quadrupole and multiple-collector ICP-MS. *Chem. Geol.* 247 (1-2), 100–118. doi:10.1016/j.chemgeo.2007.10.003
- Zhang, C., and Huang, X. (1992). The ages and tectonic settings of ophiolites in west Junggar, Xinjiang. *Geol. Rev.* 38 (6), 509–524.
- Zhang, C., Santosh, M., Liu, L. F., Luo, Q., Zhang, X., and Liu, D. D. (2018). Early Silurian to Early Carboniferous ridge subduction in NW Junggar: evidence from geochronological, geochemical, and Sr-Nd-Hf isotopic data on alkali granites and adakites. *Lithos* 300 (13), 314–329. doi:10.1016/j.lithos.2017.12.010
- Zhang, L. C., Wan, B., Jiao, X. J., and Zhang, R. (2006). Characteristics and geological significance of adakitic rocks in copper-bearing porphyry in Baogutu, West Junggar. *China Geol.* 33 (3), 626–631.
- Zhang, L. F. (1997). The  $^{40}\text{Ar}/^{39}\text{Ar}$  age of the tangbale glaucophane schist in western junggar, xinjiang and its geological significance. *Geol. Bull. China.* 42 (20), 2178–2181. doi:10.1360/csb1997-42-20-2178
- Zhang, X., and Zhang, H. (2014). Geochronological, geochemical, and Sr–Nd–Hf isotopic studies of the Baiyanghe A-type granite porphyry in the Western Junggar: implications for its petrogenesis and tectonic setting. *Gondwana Res.* 25 (4), 1554–1569. doi:10.1016/j.gr.2013.05.023
- Zhang, Y. Y., and Guo, Z. J. (2010). New constraints on formation ages of ophiolites in northern and comparative study on their connection. *Acta Petrol. Sin.* 26 (2), 421–430.
- Zheng, Y. F., Li, S. G., and Chen, J. F. (1998). Chemical geodynamics. *Adv. Earth Sci.* 13 (2), 121–128.
- Zhou, T., Yuan, F., Fan, Y., Zhang, D. Y., Cooke, D., and Zhao, G. C. (2008). Granites in the sawuer region of the West junggar, xinjiang province, China: geochronological and geochemical characteristics and their geodynamic significance. *Lithos* 106 (3), 191–206. doi:10.1016/j.lithos.2008.06.014
- Zhu, Y. F., Chen, B., Xu, X., Qiu, T., and An, F. (2013). A new geological map of the western Junggar, north Xinjiang (NW China): implications for Paleoenvironmental reconstruction. *Episodes* 36 (3), 205–220. doi:10.18814/epiugs/2013/v36i3/003
- Zhu, Y. F., He, G. Q., and An, F. (2007). Geological evolution and metallogeny in the core part of the Central Asian metallogenic domain. *Geol. Bull. China* 26 (9), 1167–1177. doi:10.3969/j.issn.1671-2552.2007.09.018
- Zhu, Y. F., and Xu, X. (2006). The discovery of early Ordovician ophiolite mélange in Taerbahatai Mts., Xinjiang, NW China. *Acta Petrol. Sin.* 22 (12), 2833–2842.